ELSEVIER

Journal of Crystal Growth 200 (1999) 435–440

JOURNAL OF CRYSTAL GROWTH

Solubility of $YBa_2Cu_3O_{7-\delta}$ and $Nd_{1+x}Ba_{2-x}Cu_3O_{7\pm\delta}$ in the BaO/CuO flux

C. Klemenz*, H.J. Scheel

Cristallogenèse, Institute of Micro- and Optoelectronics, Swiss Federal Institute of Technology, Ch. de Bellerive 34, CH-1007 Lausanne, Switzerland

Received 19 November 1998; accepted 14 January 1999
Communicated by T. Hibiya

Abstract

The knowledge of the phase relations and solubilities in the Y–Ba–Cu–O and Nd–Ba–Cu–O systems are of fundamental importance for crystal growth and liquid-phase epitaxy of $YBa_2Cu_3O_{7-\delta}$ (YBCO) and $Nd_{1+x}Ba_{2-x}Cu_3O_{7\pm\delta}$ (NdBCO). The determination of the solubility curve of YBCO and NdBCO in a BaO/CuO flux containing 31 mol% BaO was done by observation of the formation and dissolution of crystals on the surface of the high-temperature solution. The heat of the solution of YBCO at 1000°C was found to be 34.7 kcal/mol, and for NdBCO at 1060°C, it was found to be 28.1 kcal/mol. The determination of the solubility curves requires special care, and the problems of the time-dependent shift of the solution composition due to the corrosion of the crucible is discussed. The scatter of the solubility data published by different authors could be due to the use of solutions with different Ba : Cu ratios, different determination methods, i.e. different crystallization mechanisms, different crucibles and starting chemicals.

PACS: 64.75; 65.50; 81.10

Keywords: High-T_c superconductors; REBCO; Solubility; Crucible corrosion

1. Introduction

Finding a suitable solvent for a given crystal may sometimes represent a real challenge. From the solubility point of view, the optimum choice is a solvent which is chemically similar (in the type of bonding) to the solute, but this favors mutual solid-solubility. Therefore, sufficient chemical and crystal-chemical differences between the solvent and solute constituents are required in order to minimize the incorporation of solvent species into the solute structure. These crystal-chemical differences are established by differences in ionic size or in the stable valency state at growth temperature.

In the case of YBCO and NdBCO, attempts to use usual fluxes (Ba and Li-borates, lead oxide, lead fluoride, etc.) were not successful [1]. Therefore,

*Corresponding author. Tel.: + 41-21-6934393; fax: + 41-21-6934750.
E-mail address: christine.klemenz@imo.dp.epfl.ch (C. Klemenz)

0022-0248/99/$ – see front matter
PII: S0022-0248(99)00063-9

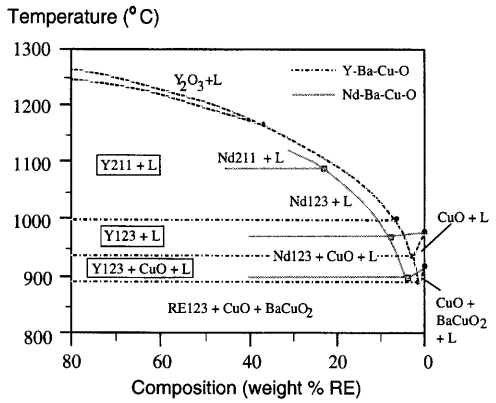

Fig. 1. Pseudobinary cut in the phase diagrams of YBCO compared with NdBCO.

a solution composition near the binary eutectic between $BaCuO_2$ and CuO, which is at about 29 ± 1.5 mol% BaO at a temperature of 910 ± 10°C in air [2], was chosen as solvent.

The two systems NdBCO and YBCO are not fundamentally different. NdBCO, compared to YBCO, has two advantages for crystal growth and liquid-phase epitaxy LPE: a higher thermal stability reaching nearly 1100°C in air, and a much wider primary crystallization field PCF, allowing concentrations up to 20 wt% for single-phase growth. Fig. 1 shows a pseudobinary cut in the phase diagrams of YBCO compared with NdBCO [3]. A disadvantage for NdBCO, however, is the solid-solubility behavior leading to deviations of the 1 : 2 Nd : Ba ratio in the crystals.

2. Solubility curve determination

The experimental determination of the solubility curve for YBCO and NdBCO was done in a chamber furnace [3]. The starting chemicals Y_2O_3 (4 N) for YBCO, or Nd_2O_3 (4 N) for NdBCO, CuO (5 N), and BaO_2 (2 N) were hand mixed and introduced in a ceramic crucible (Al_2O_3 in earlier experiments, ZrO_2 for the refined solubility curve). The temperature gradient in the furnace was set in such a way that the "coldest" place was the middle of the surface of the solution, and no crystallization occurs at the crucible walls or on the crucible bottom. After

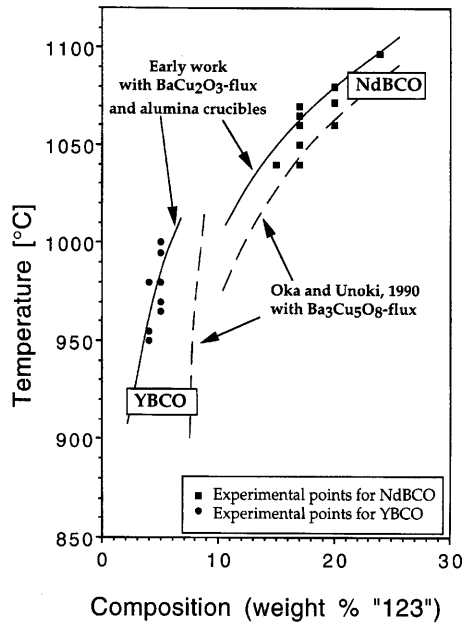

Fig. 2. Early solubility curves of YBCO and NdBCO from our work [1]. The scatter of data is mainly due to the corrosion of the alumina crucibles.

soaking and homogenization of the solution, the formation and dissolution of the crystals could be observed by inducing small temperature changes by shifting a ceramic piece at the top of the furnace. Once a small crystal formed, which could easily be observed, and did not grow further for few hours, we concluded that the solution was equilibrated and this gave one point on the solubility curve. Solutions with different starting amounts of REBCO (RE = Y, Nd) were prepared, and by this way the solubility curves for NdBCO and YBCO were obtained, as shown in Fig. 2.

In the phase diagram, the solubility curve is located on a surface (on the primary crystallization field), and will therefore vary as a function of the Ba/Cu ratio, i.e. the composition of the solution. This Ba/Cu ratio depends not only on the starting composition of the solution, but also on the crucible corrosion problems. Effectively, in early experiments, we used Al_2O_3 crucibles [3], and obtained a strong scatter of the results (see Fig. 2). This was attributed to the strong corrosion of the alumina crucibles, which produces a time and temperature-dependent shift in the solubility curve,

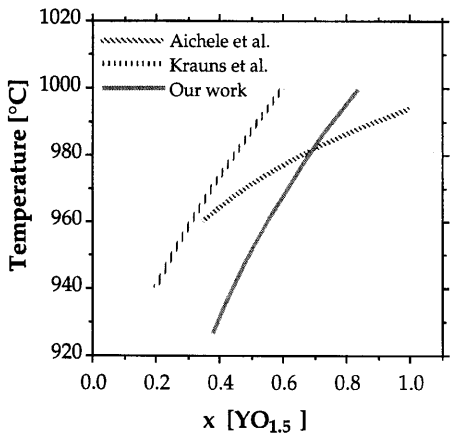

Fig. 3. Comparison between our refined solubility data for YBCO in the BaO/CuO flux at 31 mol% BaO and the data of Aichele et al. [11] and Krauns et al. [12].

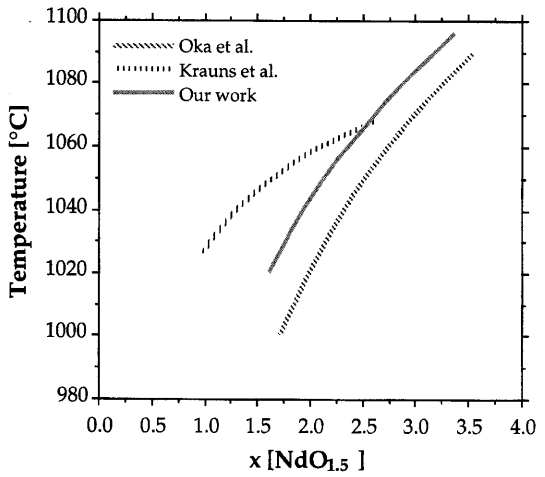

Fig. 4. Comparison between our refined solubility data for NdBCO in the BaO/CuO flux at 31 mol% BaO and the data of Krauns et al. [12] and Oka et al. [19].

by changing the composition of the solution, and to the difficulties of HTSCs [4].

After recognition of these crucible corrosion problems and optimization of the process, the solubility curves of YBCO and NdBCO could be refined. Fig. 3 show the Arrhenius fit to our refined solubility data for YBCO, and Fig. 4, for NdBCO, compared with solubility data of other authors.

One should also mention, that the metastable (Ostwald Miers) region did not represent a problem in determining the liquidus curve by observation of crystallization on top of the solution, for this system, which might not be valid for other crystal/solvent systems.

Our solubility curves were further tested by LPE experiments: nonpolished $NdGaO_3$(1 1 0) substrates for YBCO, and nonpolished $LaGaO_3$(0 0 1) substrates for NdBCO were dipped into the solution of defined composition at decreasing temperatures. The temperature at which epitaxial deposition occurred was considered as near-liquidus temperature. There was a difference between the temperature at which epitaxy was obtained and the temperature at which crystals were formed at the top of the solution, but the observed variations were small, lying in the range of 1–3°C.

3. Heat of solution

There exist different possibilities to express the heat of solution. One can tentatively assume the phase transition (one-particle model) between the solid (s) and liquid (l) REBCO phase:

$$REBa_2Cu_3O_{7-x(s)} \rightleftharpoons REBa_2Cu_3O_{7-y(l)}$$

with a different oxygen content in the liquid and in the solid phases.

Assuming an ideal solution, the relationship between the concentration, expressed in mol fraction, x_1 and x_2 at the temperatures T_1 and T_2, respectively, would then be given by

$$\ln\left(\frac{x_2}{x_1}\right) = -\frac{\Delta H_{fus}}{R}\left(\frac{1}{T_2} - \frac{1}{T_1}\right), \quad (1)$$

where ΔH_{fus} is the fusion enthalpy (or heat of fusion). For an ideal solution, a linear plot of $\ln(x)$ versus $1/T$ is obtained, and this Arrhenius-type relation allows to extrapolate the whole solubility curve from the melting point of the solute and a few solubility data. A deviation from linearity would indicate nonideal solution behavior. Since the volume change on melting is small, ΔH_{fus} can be approximated by the heat of solution (or heat of dissolution) L_{sol} [5,6], which is related to the saturation concentration of the solute in the solvent by

the relationship

$$L_{sol} = RT^2 \, d\ln x_{sat}/dT, \quad (2)$$

or

$$L_{sol} = 4.574 T_1 T_2 \frac{\log x_{sat1} - \log x_{sat2}}{T_1 - T_2}, \quad (3)$$

where x_{sat1} and x_{sat2} are the saturation concentrations at temperatures T_1 and T_2, respectively.

Using the above expressions and according to our refined experimental solubility curve, for $YBa_2Cu_3O_{7-x}$ crystals with $x \approx 0.8$, grown in air ($P_{O_2} = 0.2$ atm) in a flux with a Ba : Cu ratio of 31 : 69, we obtain $L_{sol} = 34.7$ kcal/mol at 1273 K [7]. This value is in good agreement with the data of Tsagareisvili et al. [8,9] who give for the enthalpy of fusion ΔH_{fus} of $YBa_2Cu_3O_6$ at 1446 K a value of 36.44 kcal/mol and for $YBa_2Cu_3O_7$ at 1503 K a value of 41.03 kcal/mol. For $Nd_{1.1}Ba_{1.9}Cu_3O_{7+\delta}$ [10] crystals grown in air, at 1060°C, from the same flux composition, we obtain $L_{sol} = 28.1$ kcal/mol at 1333 K.

Different values for the heat of solution of YBCO [11,12] and NdBCO [12] can be found in the literature. The scatter of the data could be explained by the use of another solvent composition, different starting chemicals (purities), crucibles, and determination method, as will be discussed further below.

The heat of solution can also be expressed by using a multi-particle model, similar to the eight particle model used for garnets [13–16]. In this case, it is assumed that the REBCO molecule splits into several particles or molecules upon dissolution according to

$$REBa_2Cu_3O_{7-x(s)} \rightleftharpoons Y^{3+} + 2Ba^{2+} + 3Cu^{2+} + (7-x)O^{2-}$$

or

$$REBa_2Cu_3O_{7-x(s)} \rightleftharpoons YO_{1.5(l)} + 2BaO_{(l)} + 3CuO_{(l)}$$

This latter expression was used in an attempt to fit solubility data of different authors [11].

For our considerations, the one-particle model was preferred, since the heat of solution expressed by this way allows the theoretical determination of growth parameters in liquid-phase epitaxy LPE of YBCO [7,17], where unit-cell growth is assumed, and a good fit with experimental results was found.

4. Shift of the solubility curve

Several reasons may lead to a shift of the solubility curve. The first is the crystallization of YBCO or NdBCO itself, depending on the flux composition. The Ba : Cu ratio 3 : 5 has been chosen as solvent [12], for experiments involving the peritectic decomposition of the Y_2BaCuO_5 (211 phase) into YBCO (123 phase), because the composition of the flux does not change during crystallization/dissolution of the 211 and 123 phases. In our experiments, the volume of the crystallites formed at the top of the solution is very small with respect to the volume of the solution. Therefore, the variation of the solution composition can be neglected.

Another reason to observe a shift in the liquidus temperature with time, is the crucible corrosion. For alumina crucibles, corrosion by the $BaCuO_2$/CuO-flux starts with the diffusion of Ba and Cu ions into the alumina, followed by the formation of a Cu-containing barium-aluminate layer. After saturation of the crystal-growth solution, the aluminate may be deposited in crystalline form at the other solid boundaries. Depending on the crucible manufacturer, Al-containing phases are crystallizing after few days only, giving a solution saturated with alumina.

In comparison to alumina crucibles, zirconia crucibles are less corroded by the $BaCuO_2$/CuO melt. ZrO_2 crucibles have to be stabilized with 5–15% Y_2O_3 or CaO, in order to suppress the crystallographic phase transition of ZrO_2. For these crucibles, the reaction layer consists of Y, Ca, Cu-containing $BaZrO_3$, depending on the sintering aids used by the manufacturer. The thickness of this reaction layer increases with time, and the viscosity of the solution increases continuously, modifying the solution composition. For our determination of the solubility curve, however, these crucibles could be used, since their corrosion rate is relatively low (about 10 times lower than for Al_2O_3, see below), and the crystallization of YBCO or NdBCO was

observed latest one day after complete dissolution of the starting oxides.

The use of Y_2O_3 and Nd_2O_3 crucibles for the determination of the solubility curve of YBCO and NdBCO, respectively, are not suitable, except if the method used by Krauns et al. [12] is applied. By using yttria crucibles, one has a self-saturation system: the Y^{3+} ions are continuously supplied from the crucible wall, until the solution is saturated.

The corrosion velocity depends on the manufacturer, and may vary depending on different factors, such as porosity or sintering aids used. We measured the corrosion velocity of our Al_2O_3, ZrO_2, and Y_2O_3 crucibles after different runs, and the results agreed to former measurements [18].

The effect of crucible corrosion on the solution composition is shown in Fig. 5, assuming a cylindrical crucible in which the height in contact with the melt corresponds to the crucible diameter, offering a surface of 92 cm^2 in contact with the melt. In this figure, for simplification, the liquidus curves are shown as straight lines. For Al_2O_3 crucibles, the mean corrosion velocity in the first 24 h was 27 μm/h. Thus, in 24 h, the solution composition shifts from 30 to 24.6 mol% BaO (or from 31 to 25.8 mol% BaO). For ZrO_2 crucibles, the mean corrosion velocity in the first 24 h was 2.1 μm/h, which represents a shift in the solution composition from 31 to 30.54 mol% BaO, and after ten days, the solution composition shifts from 31 to 28.40 mol% BaO. The mean corrosion velocity of the Y_2O_3 crucibles in the first 24 h was 3.2 μm/h, and in 24 h, the solution composition shifts from 31 to 30.54 mol% BaO.

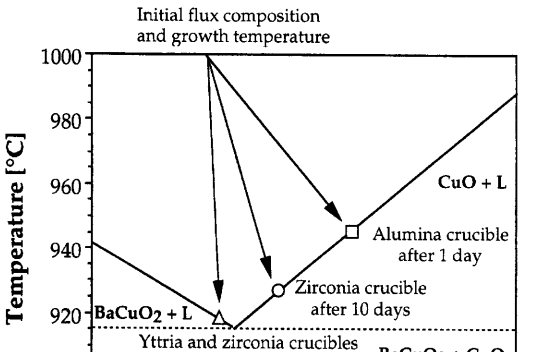

Fig. 5. Change of flux composition as a function of time, due to crucible corrosion, for the mean corrosion rates of 27 μm/h for alumina, 2.1 μm/h for zirconia, and 3.2 μm/h for yttria crucibles.

5. Discussion and conclusions

Similar to earlier results and observations for garnets [13], there is a strong scatter in the published solubility data, as shown in Fig. 3 for YBCO [11,12] and in Fig. 4 for NdBCO [12,19]. This fact can tentatively be explained by the difficulties of HTSCs [4], by different determination methods, by different solution compositions, and different chemicals and crucibles. Aichele et al. [11] used the dipping of (1 1 0)$NdGaO_3$ substrates at different $YO_{1.5}$ concentration, using a flux with a BaO : CuO ratio of 31.3 : 68.7 and yttrium stabilized ZrO_2 crucibles, whereas Krauns et al. [12] obtained their data from dipping thermally equilibrated MgO single-crystals and relatively cold alumina rods in their solution and by analyzing the melt solidified on it. They used a BaO : CuO ratio of 37.5 : 62.5, and yttria or magnesium oxide crucibles.

For YBCO and NdBCO, the determination of the solubility by dipping $NdGaO_3$ and $LaGaO_3$ substrates in the solution, could be applied, since the variations with respect to the results obtained from observations of crystal formation on top of the solution were small. But one has to be careful with the determination of a liquidus curve only by dipping substrates (or polycrystalline materials) in a solution, without observation of crystallization, since it is not guaranteed that crystallization occurs on the substrate *only*. By observation of crystallization at the top of the solution, by taking out the as grown crystals for analysis, and by decanting the flux, it is relatively easy to detect any secondary crystallization at the crucible wall or bottom and to confirm the crystallization of the right phase. The supersaturation needed for nucleation and initial growth depends on the substrate parameters. With increasing misfit, the supersaturation has to be increased [20], and with increasing substrate misorientation, it will be lower, since more substrate

steps (and kinks) will be available. Furthermore, the supersaturation depends on the substrate composition (chemical and thermal stability), the crystallographic orientation of the substrate, and on the roughness of the substrate surface.

Depending on the crystal/solution system, and the growth temperature, interface reactions (between substrate and solution) may influence the obtained results. In the case of YBCO, for example, the use of (1 1 0)$NdGaO_3$ is not so easy: very close to the liquidus temperature, the $NdGaO_3$-substrate is etched [21], which increases the supersaturation close to the interface [7,17], and a (Y,Nd)BCO layer is obtained. It needs some training to recognize (by Nomarski differential interference contrast microscopy) whether the thin grown layer is YBCO, or whether etching occurs. Thus, chemical analysis is needed.

For the $Nd_{1+x}Ba_{2-x}Cu_3O_{7+\delta}$ system, problems may arise from the solid-solubility behavior. Thus, the value of x may depend on the Ba : Cu ratio, the temperature, and the oxygen partial pressure. For NdBCO, our solubility data show a large difference from the data of Krauns et al. [12], whereas for YBCO, the fit is better, if one assumes that a lateral shift of the solubility curve is easier to explain with respect to a different (but constant) Ba : Cu ratio. However, it is rather difficult to believe that the scatter of published data are only due to compositional factors and further investigations are required in order to understand by which way crystallization and dissolution mechanisms of REBCO occur for the different cases, and their impact on the determination of the solubilities.

Acknowledgements

The authors would like to thank P. Holba for fruitful discussions. Financial support by the Swiss National Science Foundation (project 21-43'437.95) and by the US Army/European Office (contract N68171-96-C-9105) is gratefully acknowledged.

References

[1] H.J. Scheel, F. Licci, J. Crystal Growth 85 (1987) 607.
[2] F. Licci, H.J. Scheel, P. Tissot, J. Crystal Growth 112 (1991) 600.
[3] C. Klemenz, H.J. Scheel, J. Crystal Growth 129 (1993) 421.
[4] H.J. Scheel, F. Licci, Thermochim. Acta 174 (1991) 115.
[5] P. Bennema, J.P. van der Eerden, in: I. Sunagawa (Ed.), Morphology of Crystals, Terra Scientific Publishing Company, Tokyo, 1987 (Chapter 1).
[6] G.H. Gilmer, K.A. Jackson, in: E. Kaldis, H.J. Scheel (Eds.), Crystal Growth and Materials, North-Holland, Amsterdam, 1977.
[7] C. Klemenz, H.J. Scheel, Physica C 265 (1996) 126.
[8] D.Sh. Tsagareishvili, G.G. Gvelesiani, I.B. Baratashvili, G.K. Moiseev, N.A. Vatolin, Russ. J. Phys. Chem. 64 (1990) 1404.
[9] G.K. Moiseev, N.A. Vatolin, S.I. Zaizeva, N.I. Ilyinych, D.S. Tsagareishvili, G.G. Gvelesiani, I.B. Baratashvili, J. Sestàk, Thermochimica Acta 198 (1992) 267.
[10] C. Klemenz, J. Crystal Growth, in preparation.
[11] T. Aichele, S. Bornmann, C. Dubs, P. Gornert, Cryst. Res. Technol. 32 (1997) 1145.
[12] C. Krauns, M. Sumida, M. Tagami, Y. Yamada, Y. Shiohara, Z. Phys. B 96 (1994) 207.
[13] W. Tolksdorf, F. Welz, Crystal growth of magnetic garnets from high-temperature solutions, in: C.J.M. Rooijmans (Ed.), Topics in Crystal Growth, Vol. 1, Springer, Berlin, 1978.
[14] W. van Erk, J. Crystal Growth 43 (1978).
[15] W. van Erk, J. Crystal Growth 46 (1979) 539.
[16] W. van Erk, J. Crystal Growth 57 (1982) 71.
[17] C. Klemenz, J. Crystal Growth 187 (1998) 221.
[18] M. Berkowski, P. Bowen, T. Liechti, H.J. Scheel, J. Am. Ceram. Soc. 75 (1992) 1005.
[19] K. Oka, H. Unoki, J. Crystal Growth 99 (1990) 922.
[20] M.H. Grabow, G.H. Gilmer, Surf. Sci. 194 (1988) 333.
[21] C. Dubs, T. Schüler, G. Bruchlos, M. Zeisberger, P. Görnert, J. Crystal Growth 156 (1995) 216.